Received: 12 August 2021 | Revised: 15 December 2021 | Accepted: 21 December 2021

DOI: 10.1111/vru.13073

IMAGING DIAGNOSIS

WILEY

Diagnosis and radiation therapy of an extensive myxoma in the retropharyngeal region infiltrating the cranial cervical vertebral canal in a dog

David Schmid[1] | Maximilian Körner[2] | Carla Rohrer Bley[2]

[1] Clinic of Diagnostic Imaging, Vetsuisse Faculty, University of Zurich, Zurich, Switzerland

[2] Division of Radiation Oncology, Vetsuisse Faculty, University of Zurich, Zurich, Switzerland

Correspondence
David Schmid, Clinic for Diagnostic Imaging, Vetsuisse Faculty, University of Zurich, Winterthurerstrasse 258c, CH-8057 Zurich, Switzerland.
Email: daschmid2@vetclinics.uzh.ch

[Correction added on 18 May 2022, after first online publication: CSAL funding statement has been added.]

Abstract

An 8-year-old, intact Rottweiler-female dog presented due to an acute onset of lethargy, abnormal gait, and wheezing. Physical examination revealed stridor, cervical pain, and ambulatory tetraparesis. Magnetic resonance imaging-examination displayed a lobulated, fluid-filled mass extending from the sphenoid bone to C5, infiltrating the cranial vertebral canal causing extradural compression of the spinal cord and narrowing of the pharynx. An emergency debulking-surgery around the pharynx was performed. Histopathological findings were consistent with a myxoma. The remaining tumor was irradiated resulting in stable disease 6 months later. The dog died 18 months later due to aspiration pneumonia without clinical signs of neurologic or respiratory compromise.

KEYWORDS
canine, irradiation, MRI, retropharyngeal mass, synovial

1 | SIGNALMENT, HISTORY, CLINICAL FINDINGS

An 8-year-old female intact Rottweiler was referred due to a history of progressive wheezing, with onset noticed 8 months before presentation. A CT examination (Activion 16-slice CT, Toshiba, Tustin, CA; pre- and postcontrast administration Accupaque™ 300, 300 mg Iod/ml, GE Healthcare AG, Opfikon) performed by the referring clinic showed a large, well-defined, extensive, lobulated space-occupying lesion in the retropharyngeal region. This lesion caused moderate mass effect to the surrounding tissue and extended into the vertebral canal at the level of C1-C2 causing mild extradural spinal cord compression.

In the initial clinical examination, vital parameters were within normal limits. The dog was lethargic and an inspiratory stridor and moderate swelling in the laryngeal area were noticed. At this time point, no neurological deficits were reported. The lesion was sampled under ultrasound guidance and a clear, viscous fluid was aspirated. Cytological analysis revealed the fluid as mildly eosinophilic material with a moderate number of macrophages as it can be seen in saliva.

The findings were considered to be compatible with a non-neoplastic cyst like a sialocele.[1] Bilateral sialoadenectomy of the sublingual and mandibular salivary glands was performed. Histology of the salivary glands was interpreted as mild, chronic, plasma-cellular sialadenitis.

Four weeks later, the dog presented to the emergency service because of an acute onset of neck pain. Furthermore, the wheezing and laryngeal swelling had worsened despite surgical treatment. On neurological examination, a mild ambulatory tetra-paresis with reduced proprioception of all four legs was found. Reflexes were normal. Manipulation of the neck caused severe pain reaction. Based on the clinical signs, the neuroanatomical localization was C1-5. A complete blood count,

Previous presentation or publication disclosure: The content of this study has not been previously presented or published.

Equator network disclosure: A CARE checklist has been used.

blood chemistry, and chest radiographs in two lateral projections, all unremarkable, completed the clinical examination.

2 | IMAGING, DIAGNOSIS, AND SURGICAL TREATMENT

Due to the clinical findings and previous CT findings indicating extramedullary spinal cord compression, expansion of the lesion was suspected and therefore MRI of the cervical vertebral column was performed under general anesthesia using a 3-Tesla-scanner (Philips Ingenia, Philips AG, Zurich, Switzerland; MRI acquisition protocol see Appendix 1, Table S1).

The lobulated retropharyngeal space occupying lesion had expanded compared to the CT examination with extension from the area of the sphenoid bone to the caudal aspect of C5. A marked mass effect on the surrounding soft tissue was visible, with ventral displacement of the larynx, trachea, and esophagus and almost complete narrowing of the pharynx. The lesion had progressively expanded and invaded the paravertebral soft tissue of the atlanto-occipital region and infiltrated the cranial vertebral canal. Within the vertebral canal, the extradural portion extended from the occiput to the cranial third of C2 with involvement of all atlanto-occipital and atlantoaxial joint cavities.

The space-occupying lesion displaced the brainstem and the spinal cord left-dorsally, accentuated at C1-C2. The spinal cord and brainstem showed normal signal intensity. The mass was predominantly composed of lobulated material of fluid signal intensity separated by thin septae. This fluid was isointense to CSF in all sequences. The lesion showed mild rim enhancement and mild enhancement of the described septae following administration of contrast. The parotid salivary gland was unremarkable on both sides, without visible contact to the lesion (see Figure 1).

After the acquisition of the MRI images, the dog's neurological status deteriorated (non-ambulatory tetra-paresis), with severe pain and severe dyspnea. An emergency surgery consisting of decompression of the upper airways and placement of a Blake drain (Blake™ Silicone Drains, Ethicon, Inc., Sommerville, New Jersey, USA) was carried out. Intraoperatively, the lesion presented as a lobulated, greyish mass with fine septae, filled with clear mucoid fluid. The lesion was growing between the fascial planes of the cervical muscles and was firmly attached to the adjacent anatomic structures. Therefore, debulking was only feasible in areas where the surrounding tissue could be partially removed. Due to proximity of the lesion to the brainstem and suspected adhesion of the lesion to the surrounding tissue, the cervical part of the lesion was not approached surgically.

Postoperative treatment consisted of pain medication, corticosteroids, gastroprotectant, and supplemental O_2 (full medical treatment see Appendix 2). Surgically excised material was processed for histologic examination. In fresh frozen sections, the entire mass consisted of a mucinous to collagenous matrix, surrounding small spindle to stellate cells with hyperchromatic nuclei. In the regular processed paraffin-embedded slices the same neoplastic cells were observed, forming nodules and streams, which appeared to infiltrate the presumed preexisting collagenous to adipose tissue, showing the neoplasm as a nonencapsuled lesion of low cellularity. Cells were small with scant pleomorphism and no mitoses were observed. The histopathological diagnosis was an infiltrative myxoma.

3 | RADIATION THERAPY AND OUTCOME

Radiation therapy (RT) of the tumor and the scar tissue started 14 days after the debulking-surgery. The treatment was delivered on a Monday to Friday schedule. Planning-CT and daily treatments were performed in dorsal recumbency under general anesthesia. Reproducible positioning was accomplished with both an individually shaped vacuum cushion (BlueBag BodyFix, Elekta AB, Stockholm, Sweden) and a custom-made bite block. Contouring and treatment planning was performed using Eclipse External Beam Planning system version 15.1 (Varian Oncology Systems, Palo Alto, USA) with the Anisotropic Analytical Algorithm (AAA) (15.1.51).

Contouring of organs at risk (OAR) and target volumes were performed on co-registered postcontrast CT images from the planning-CT in order to increase accuracy of contouring. Tongue, spinal cord, larynx/trachea, esophagus, and brain were defined and contoured as OAR. Radiation was planned isocentrically, with heterogeneity correction and delivered with a 6 MV linear accelerator (Clinac iX, Varian, Palo Alto, California) equipped with a 5-mm multi-leaf-collimator, using photons and intensity-modulated radiation therapy. Daily image-guidance (IGRT) was used for treatment verification, using kV-kV orthogonal radiographs and/or kV cone-beam CT (CBCT).

The dose was prescribed at the ICRU reference point, delivered in a protocol of 20×2.25 Gy (total dose of 45 Gy). The dose was normalized to ensure that $\geq$98% of the PTV was covered by the 95% isodose line (for dose statistics see Appendix 3, Table S2). During RT a drain had to be placed due to severe fluid- and mucus-production in the retropharyngeal area resulting in recurrent stenosis of the upper airways. After partial fluid removal, the treatment plan was adapted to the new target volumes. The drain stayed in place for 3 weeks and was removed 3 days after the last radiation session.

Two months following RT, a short-protocol, non-contrast-enhanced MRI control was performed. The lesion within the vertebral canal was unchanged in size; the retropharyngeal portion of the myxoma showed a moderate decrease in volume with reduced mass effect to the surrounding tissue. Six months post-RT, the dog was in good general condition. The neurological examination revealed a mild ambulatory tetraparesis with mildly reduced proprioception of all four legs and normal reflexes. No pain reaction could be evoked during neck manipulation.

At this time point a follow-up MRI examination of the retropharyngeal area and the cervical vertebral column was conducted using an identical protocol as in the initial MRI examination (see Figure 2). The portion within the vertebral canal was unchanged in the follow-up MRI study 2 and 6 months after irradiation (pre-RT: 12.7×8 mm vs. 2 months post-RT: 13.5×7.9 mm vs. 6 months post-RT: 14.4×6.2 mm [length $\times$ height in mm; measured in transversal T2 sequences]). The

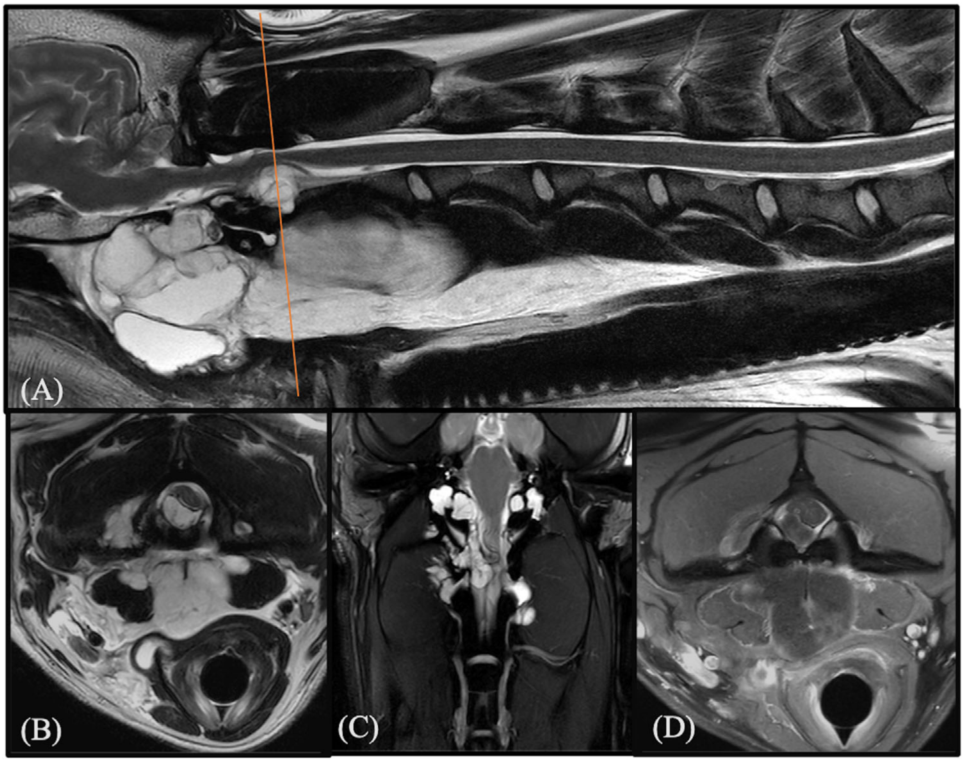

FIGURE 1 Initial MRI examination. Sagittal T2 weighted image **(A)** showing the severe expansion of the space occupying lesion with fluid intensity in the retropharyngeal area and the resulting severe ventral compression of the pharynx. The infiltration of the vertebral canal at the level C1-C2 and the proximity to the brainstem can be noted in the dorsal T2 weighted (SPIR) image **(C)**. The resulting moderate compression of the spinal cord and brainstem is depicted in the transverse T2-weighted image **(B)** and transverseT1-weighted image following administration of contrast **(D)** [Color figure can be viewed at wileyonlinelibrary.com]

part of the myxoma within the vertebral canal was considered "stable disease" based on the response criteria for solid tumors in dogs (RECIST; classified < 30% decrease and < 20% increase in tumor volume).[2] Eighteen months after the end of the RT the dog died from a severe aspiration pneumonia. According to the owner, the dog showed no clinical changes despite the consistent mild toe dragging until the sudden onset of respiratory distress.

4 | DISCUSSION

Myxoma originates from fibroblasts and is an uncommon neoplasia in dogs.[3,4] Reported locations in dogs include subcutis, cardiac valves, odontogenic, and synovial tissue.[5,6,7,8] Synovial myxomas mostly occur in large-breed, middle-aged dogs, especially Doberman Pinschers and Labrador Retrievers.[9,8] Commonly affected locations are stifle and digit, followed by tarsus, elbow, and carpus.[8,4] A case series describes several orbital myxoma/myxosarcomas possibly arising from the temporo-mandibular joint.[10] Few reports describe myxomas associated with the articular process joints.[11,12] Only one case of a myxoma associated with the cervical vertebral column is reported.[13] Another report presents a similar case with the more malignant variant, a cervical myxosarcoma.[14] As described in previous reports of synovial myxoma of articular process joints, the tumor showed a myxoid matrix with extremely low and high signal intensity on T1- and T2-weighted MRI, respectively, a lobulated appearance, mild rim enhancement, and an infiltrative character. The definite origin of this myxoma is unclear, but synovial tissue of the composite occipito-atlas-axis joint cavity seems to be most likely. The myxoma in this case showed an unusually large and ventral extension into the surrounding tissue, especially the retropharyngeal region. This unusual distribution led to misinterpretations of differential diagnoses and histopathology was essential for the final diagnosis of a myxoma.

Despite their histological benign appearance, myxomas often grow infiltratively and treatment of choice is wide surgical removal.[4] During surgical debulking of the pharynx, the myxoma presented with a highly infiltrative character, as displayed in the MRI examination, and showed marked attachment to the surrounding tissue. Therefore, adhesions were also suspected in the portion within the vertebral canal. Due to the proximity of the lesion to the brainstem, the large extent of the myxoma into the vertebral canal and poor surgical access in this area, it was decided to irradiate the tumor. After irradiation, the tumor showed no clinically detectable tumor growth or mucus production. The dog was pain-free and fully functional in all activities of daily living until the sudden onset of an aspiration pneumonia. The most likely pathomechanism leading to the aspiration pneumonia is pharyngeal dysphagia; either secondary to functional impairment of the hypoglossal nerve (XII) or due to the mass effect of the retropharyngeal portion of the

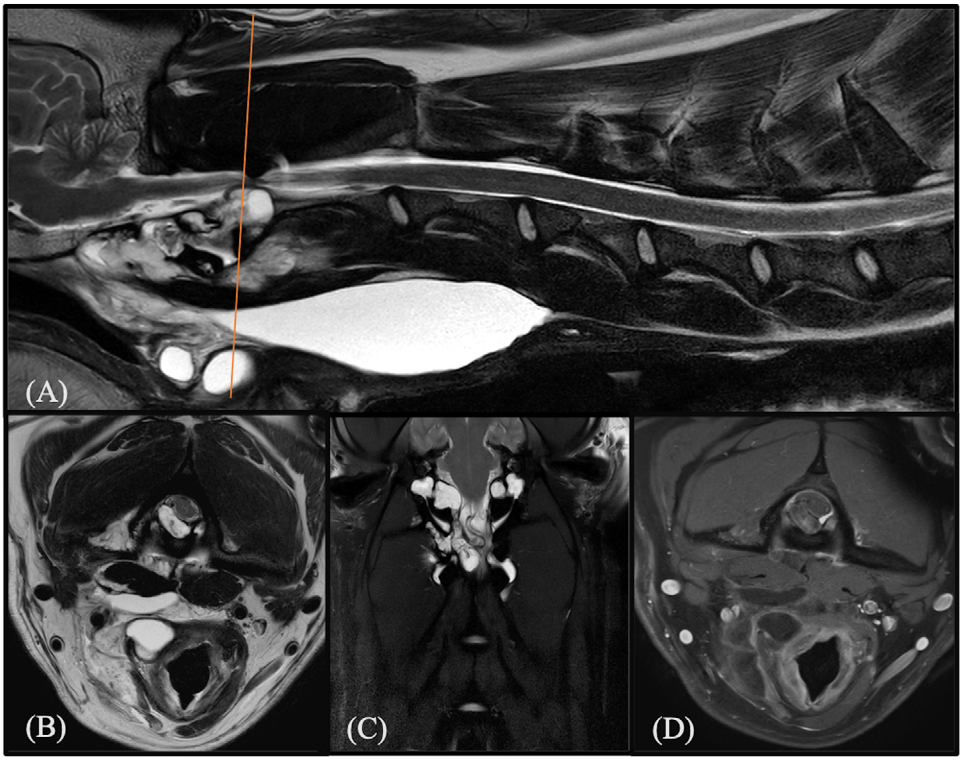

FIGURE 2 Follow up MRI examination six months post RT. The retropharyngeal extension of the space occupying lesion with fluid intensity is moderately reduced in comparison to the initial examination before surgical debulking; consequently, the lesion has a lesser mass effect to the pharynx, best seen in the sagittal T2-weighted image **(A)**. B-D, The portion within the vertebral canal remains unchanged with stationary moderate compression of the spinal cord at the level C1-C2 and mild compression of the brainstem [Color figure can be viewed at wileyonlinelibrary.com]

myxoma. In this case, irradiation was considered a useful treatment to protract recurrence and could be a possible alternative (palliative) treatment option to limb amputation in selected cases with periarticular myxomas.

LIST OF AUTHOR CONTRIBUTIONS

Category 1

(a) Conception and design: Schmid, Körner, Rohrer Bley
(b) Acquisition of data: Schmid, Körner
(c) Analysis and interpretation of data: Schmid, Körner, Rohrer Bley

Category 2

(a) Drafting the article: Schmid, Körner, Rohrer Bley
(b) Revising article for intellectual content: Schmid, Körner, Rohrer Bley

Category 3

(a) Final approval of the complemented article: Schmid, Körner, Rohrer Bley

Category 4

(a) Agreement to be accountable for all aspects of the work ensuring that questions related to the accuracy or integrity of any part of the work are appropriately investigated and resolved: Schmid, Körner, Rohrer Bley

ACKNOWLEDGMENT

Open Access Funding provided by Universitat Zurich within the CRUI-CARE Agreement.

CONFLICT OF INTEREST

The authors declare no conflict of interest.

ORCID

David Schmid https://orcid.org/0000-0002-6123-8528
Maximilian Körner https://orcid.org/0000-0001-8925-4899
Carla Rohrer Bley https://orcid.org/0000-0002-5733-2722

REFERENCES

1. Benjamino KP, Birchard SJ, Niles JD, Penrod KD. Pharyngeal mucoceles in dogs: 14 cases. *J Am Anim Hosp Assoc*. 2012; 48:31-35.
2. Nguyen SM, Thamm DH, Vail DM, London CA. Response evaluation criteria for solid tumours in dogs (v1.0): a Veterinary Cooperative Oncology Group (VCOG) consensus document. *Vet Comp Oncol*. 2015; 13(3):176-183.
3. Hendrick MJ. Mesenchymal tumors of the skin and soft tissues. In: Meuten DJ, ed. *Tumors in Domestic Animals*. John Wiley & Sons; 2016;142-175.
4. Craig LE, Thompson KG. Tumors of Joints. In: Meuten DJ, ed. *Tumors in Domestic Animals*. John Wiley & Sons; 2016;337-355.
5. Akkoc A, Ozyigit MO, Cangul IT. Valvular cardiac myxoma in a dog. *J Vet Med A Physiol Pathol Clin Med*. 2007; 54:356-358.
6. Meyers B, Boy SC, Steenkamp G. Diagnosis and management of odontogenic myxoma in a dog. *J Vet Dent*. 2007; 24:166-171.

7. Hayes AM, Dennis R, Smith KC, Brearley MJ. Synovial myxoma: magnetic resonance imaging in the assessment of an unusual canine soft tissue tumour. *J Small Anim Pract*. 1999; 40:489-494.
8. Craig LE, Krimer PM, Cooley AJ. Canine synovial Myxoma: 39 cases. *Vet Pathol*. 2010; 47:931-936.
9. Craig LE, Julian ME, Ferracone JD. The diagnosis and prognosis of synovial tumors in dogs: 35 cases. *Vet Pathol*. 2002; 39:66-73.
10. Dennis R. Imaging features of orbital myxosarcoma in dogs. *Vet Radiol Ultrasound*. 2008; 49:256-263.
11. Khachatryan AR, Wills TB, Potter KA. What is your diagnosis? Vertebral mass in a dog. *Vet Clin Pathol*. 2009; 38:257-260.
12. Blair WH, et al. Imaging diagnosis - synovial myxoma of lumbar vertebra articular process joint. *Vet Radiol Ultrasound*. 2011; 52:309-312.
13. Neary CP, Bush WW, Tiches DM, Durham AC, Gavin PR. Synovial Myxoma in the vertebral column of a dog: MRI description and surgical removal. *J Am Anim Hosp Assoc*. 2014; 50:198-202.
14. Kunkel KAR, Palmisano MP, Stefanacci JD. Imaging diagnosis- spinal myxosarcoma in a dog. *Vet Radiol Ultrasound*. 2007; 48:557-559.

SUPPORTING INFORMATION

Additional supporting information may be found in the online version of the article at the publisher's website.

How to cite this article: Schmid D, Körner M, Bley CR. Diagnosis and radiation therapy of an extensive myxoma in the retropharyngeal region infiltrating the cranial cervical vertebral canal in a dog. *Vet Radiol Ultrasound*. 2022;63:E24–E28. https://doi.org/10.1111/vru.13073